Study of Common-Mode Noise in an Electric Vehicle by Means of SPICE Simulations

Ph.D., Maurizio, Tranchero, Ideas & Motion, Italy
Paolo, Santero, Ideas & Motion, Italy
Georg, von Pfingsten, Rheinmetall AG, Germany
Mika, Nuotio, Rheinmetall AG, USA
Michael, Breuer, Rheinmetall AG, Germany

1 Introduction

Electromagnetic noise produces lots of issues in every environment, but in the automotive field the disturbances caused by each unit have to be strictly defined in order to avoid malfunctioning that might affect units related to vehicle safety and control. For this reason, international regulations define the maximum noise levels each unit can produce on board (CISPR25 [1]) and off-board (CISPR12 [2]). When designing an Electronic Control Unit (ECU) the designer should keep in mind these limits and take into account counteractions to withstand to expected noise levels, keeping the disturbance generation below such limits. Unfortunately understanding sources of noise and how it propagates within the car is not straightforward since both phenomena are deeply connected to stray parameters due to mechanical constraints and actual ECU installation. For this reason, the typical approach is to design electronics using good practice rules and then measure on a real installation which is the actual noise generated. At this point, in case of incompliance of a given norm, the designer is forced to apply external filters or to redesign the unit. This obviously lead to huge loss of time and money.
In the last years many activities have been done to create models to predict Electro-Magnetic (EM) noise and to investigate countermeasures to be applied in the early design phase. Several works have been published on the model of EM noise and on the design of EMC filter, but most of them were based on the usage of EM simulators [3]. This paper is different and aims at modeling the conducted noise in an electric vehicle only by means of SPICE models. The approach presented in this work is similar to the one described in [4], but it is more focused on the modeling of the common mode (CM) noise generation and propagation in an electric powertrain. The modelling approach presented aims at providing simple considerations and simple modeling strategies to be applied to an electric traction system in order to guide EMC design before the real system has been produced, providing a way to study EMI countermeasures in advance. Even if the present work is tailored on electric vehicle, the approach may be extended to other fields of application.

2 Modeling the Noise and its Propagation Path

2.1 The Power Inverter

This section describes how the inverter generates noise and how it propagates through the vehicle thanks to networks of parasitic components. All the models have been developed in the LTspice environment [5], due to its flexibility, the documentation available, and its widespread use.

2.1.1 Power Device

The source of EM noise is the fact that an inverter has AC nodes switching between DC rails many times per second, injecting charge to the chassis through capacitive couplings existing between the moving node and the structure of the car. For this reason, having an accurate model capable of describing how switches behave during commutation is important. The model provided by MOSFET manufacturer was not compatible with LTspice environment and was causing model instability. For this reason, we decided to recreate device behavior by using internal LTspice primitives. To compare the model provided and our implementation, we used a simplified boost circuit (Fig. 1a), hence stimulating both MOSFET and diode operations. In order to find the best

set of parameters suitable for modeling the behavior of the MOSFET in use, we used this simple iterative approach:

1) A reference simulation has been extracted from the model coming from the SiC manufacturer, using an external simulator.
2) A parametric simulation has been set up with a generic MOSFET model in LTspice [5], where at each step we were changing a different parameter.
3) At each step we were calculating the least-square error [15] between the reference simulation and the model behavior.
4) The set of parameters with lowest error has been chosen to be our parameter choice.

The model obtained fits well the behavior of both MOSFET and body diode (as can be seen in Figure 1), moreover it resulted both more stable and faster, compared to the original one.

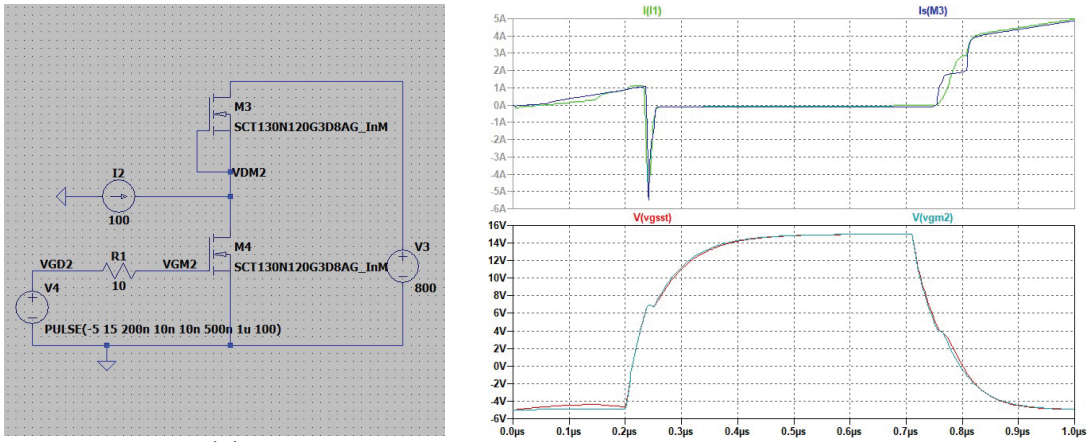

Figure 1: Our implementation of vendor's power switch: (a) LTspice circuit, comparison between the MOSFET and diode models (b).

With respect to the gate driving circuitry, it has been modelled in a very simplistic way, i.e., by using an ideal voltage source and including an external resistor to limit the slew-rate and get the dV/dt expected for this application.
The transistor and the driver has been replicated to implement a three-phase bridge and to simplify the control strategy in our model and to put ourselves into a worst case scenario, we decided to drive all the phases in a synchronous way, mimicking zero output current [6].

2.1.2 Power Module

Many works have been focused on the modeling of capacitive coupling between power module terminals and heatsinks. Dalal [7] provides a complete analysis on standard power modules that leads to a simple and effective model (Figure 2). In this case the power modules are custom and hence cannot be modeled exactly in the same way.

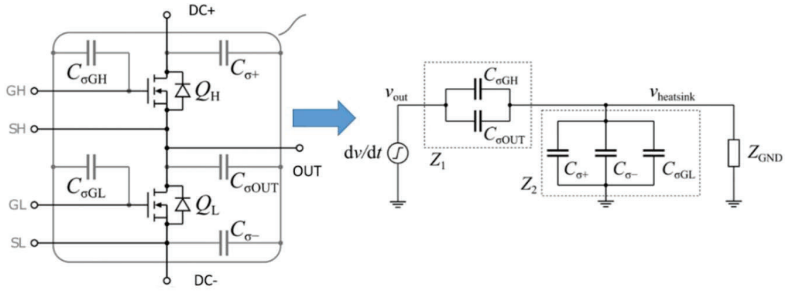

Figure 2: Capacitive coupling between power module nodes and baseplate as modelled in [7]: capacitance distribution (left) and equivalent impedance network (right).

The structure of the power module to model is shown in Figure 3-a: Two DBC substrates are hosting power devices granting a low thermal resistance towards the coolant. This structure can be modelled as a capacitor. The resulting electrical circuit including stray capacitances as shown in Figure 3-b, where the capacitive values have been extracted by a 3D solver.

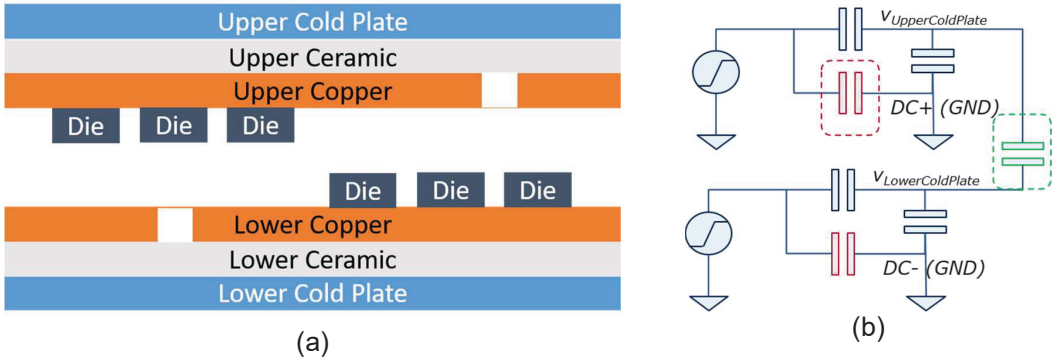

Figure 3: Structure of the custom power module (a) and its simplified stray couplings (b).

2.2 The Electric Motor

Literature on electric motor modeling is wide and introduces different level of accuracy for describing ground coupling. Martis [8] proposes a simple model phase-oriented, where each phase is modeled stand-alone as a phase inductor with a series resistance with in parallel a parasitic resistor-capacitor block modeling the input-output couplings. A stray capacitor between star-point and chassis is added to provide a path for CM currents. Bjørngreen [9] uses a more motor-oriented approach: there is a winding-to-winding capacitance, but stray resistances are neglected. Increasing the degree of complexity, we can mention Park's proposal [10] where capacitive coupling is separated in three different components: winding-to-stator, winding-to-rotor, and winding-to-winding capacitance. Next sections detail the simplified approach used in this paper.

2.2.1 Coupling

As for the power module, also in this case LTspice simulator has been used. To do that, a simplified circuit has been developed able to describe the motor accurately, but avoiding extra complexity not required by the scope of the analysis (Figure 4). The model starts from the phase inductance (L_{ph}) and phase DC resistance (R_{ph}). Then turn-to-turn capacitance is added to model coupling at high frequency (C_{tt}), moreover, each turn is naturally exposed to the stator and hence exhibits a path to chassis. Winding-to-winding coupling can be modeled modifying the turn-to-turn capacitance, adding the contribution given by the C_{ww} one, after Y-Δ transformation (see Figure 4-b).

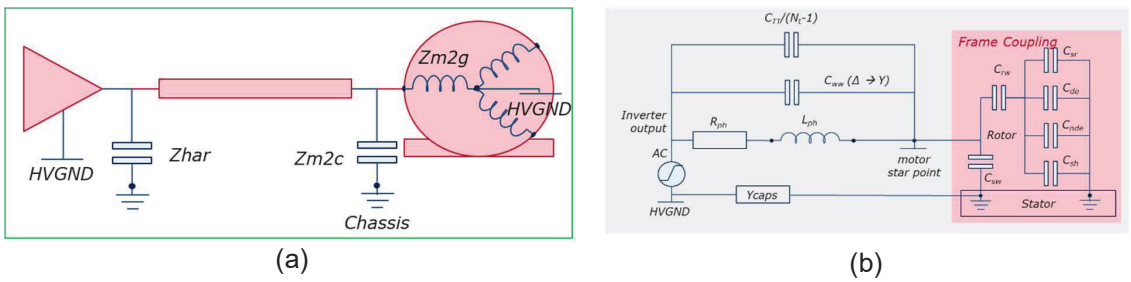

Figure 4: Coupling between parts in the electric motor (a) and its simplified implementation single and multi-stage (b).

Coupling between chassis and star-point is modeled as proposed in [11] and [12]. Looking at the measurements on the real prototypes done, it is possible to simplify this part of the circuit by considering stator-to-frame capacitance. The same is confirmed by [12]. Neglecting stator-to-rotor, rotor-to-frame, and bearings coupling, we commit a negligible error (less than 5 %).

2.2.2 Multi-stage Implementation

Electric motors have an intrinsic distributed nature since they are composed of multiple stages in series. Using a transmission line approach could be beneficial, but it might be too complex for SPICE-like simulators. To understand the need for higher order models, a parametric analysis has been done on the effects of multiple stages, keeping constant the impedance visible at external terminals (see Figure 5):

- Winding inductance (L_w) will be divided by the number of stages;
- Winding resistance (R_w) will be divided by the number of stages;
- Turn-to-turn capacitance (C_{tt}) will be multiplied by the number of stages;
- Winding-to-chassis capacitance (C_{wc}) will be divided by the number of stages;
- Resistance in series to C_{wc} (R_{wc}) will be multiplied by the number of stages.

Increasing the number of stages, we obtain a quasi-monotonic curve on CM current. After about 15 stages the current level settles to the value we can expect from an infinite number of stages (Figure 5-b). Ran [13] reports similar values (i.e., number of stages ≥ 10).

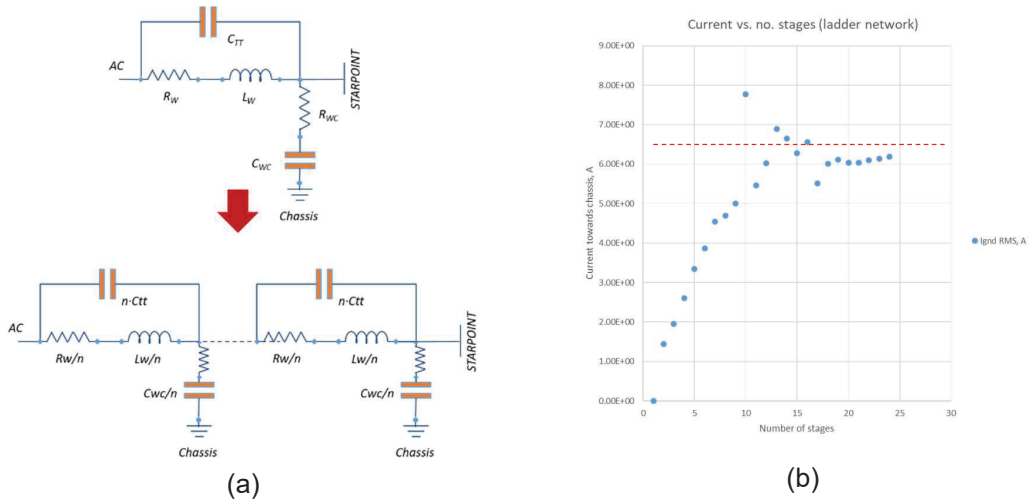

Figure 5: Single- and multi-stage simplified circuit for modeling motor coupling to chassis (a) and the CM current injected with respect to the number of stages (b).

2.2.3 Model Validation

To verify the correctness of our model, simulation results have been compared with data coming from measurements taken on the first motor samples. The focus was pointed on phase-to-chassis measurements to characterize the coupling path related to CM noise (Figure 6-a).
Looking at the model developed so far, most of the estimated parameters were correct, but the behavior above 500 kHz was not consistent with the measurements. To mimic HF behavior a stray capacitance has been added, that might be due to the interaction between motor wirings external ends. A 1-nF capacitance has been found compatible with input stage not correctly modeled by the ladder structure. This helped improving the matching at high frequency (Figure 6-b).

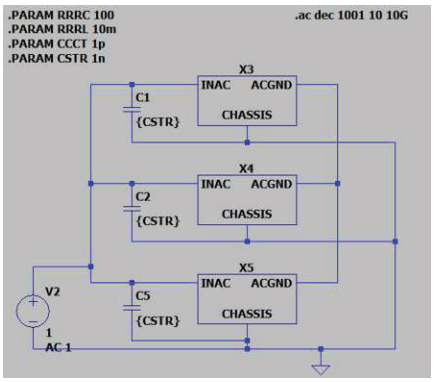

(a)

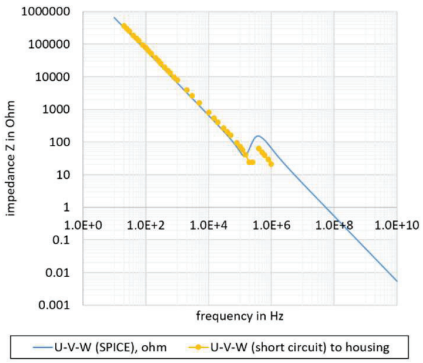

(b)

Figure 6: SPICE model used to emulate the phase-to-chassis measurement (a) and a comparison between this model and measurements on the real sample (b).

2.3 The Full System

2.3.1 Line Impedance Stabilization Network

Line Impedance Stabilization Network (LISN) are used to decouple noise produced from mains and the device under test (or vice versa) and to provide a well-known impedance to make repeatable measurements. Structure is based on LC pi network. Standard LISNs for vehicles use 5uH inductors [1]. The way the device under test is connected to the LISN is the same show in [14]. HV battery has to be maintained insulated from the rest of car for safety reasons. This well represents the scenario on a car, where all units are tightly connected to the chassis that creates a common potential among all ECUs. Since the LISN will completely decouple HV DC from the rest of the model, fine details on battery side can be avoided. This setup includes two LISNs, one for each HV DC line, each of them grounded as described by norm [1].

2.3.2 Full Model

The inverter will be modeled using a simplified half-bridge using MOSFETs based on manufacturer's model (see Sec. 2.1). Parasitic coupling between switching node and metallic plates is modeled as previously exposed (see Sec. 2.2). The three phases are modelled as one, i.e., we mimic 50% duty cycles, the worst scenario for EMC testing. This model does not take into account voltage overshooting and ringing due to current switching that can give a measurable contribution, but will not change system behavior. The motor is described using a 15-stage ladder network to emulate distributed stray inductance and capacitance introduced by windings. Value obtained by measurements on a real sample.

3 Analyses on the Model

This section describes the potentialities of the model developed in previous section, showing the possible analyses we can perform on an electric power train in the early development stage.

3.1 CM Noise

Running the model enables the estimation of the CM noise generated and propagated in the system. To analyze in frequency, the output of the simulation, a FFT has been used to extract all the harmonics composing the noise (Figure 7). The LTspice simulation has to be set up correctly to produce valid data in all frequencies under consideration, i.e., from 150 kHz to 108 MHz, please refer to [15] for further details. With 20-kHz switching frequency, a millisecond simulation requires up to 15 minutes to terminate, making this model suitable for parametric search and analyses.

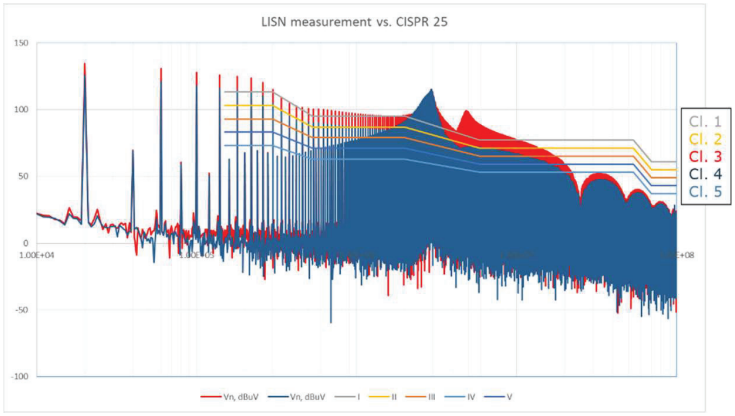

Figure 7: CM noise spectra obtained by the LTspice model described in this paper using two different Y-cap sets: 300 nF (blue) and 1 uF (red) per line. Colored lines shows the limits required by CISPR 25.

3.2 Grounding Strategies

This model has been used to investigate the best way to connect to ground these modules to reduce EMC issues by design, before realizing the real device. Power modules grounding can be configured in one of the following ways:

- connected to HV ground only, keeping high the insulation between HV and chassis;
- AC coupled with chassis, to allow noise current circulation, but preserving insulation in DC;
- connected both to HV ground and to chassis;
- completely floating, i.e., not connected either to HV ground or to chassis reference.

To analyze the effect of these grounding schemes we setup a parametric simulation where high- and low-impedances were connected between modules and chassis or HV reference to compare results.
Results can be summarized as follows:

1) Leaving power modules ungrounded produces huge voltage swings on cooling plates,
2) Asymmetries in results are caused by asymmetric capacitive paths among AC node and cooling plates.
3) Shorting currents locally, i.e., connecting power modules and the motor (using a return connection on AC cables), will deviates some current from the one circulating on chassis, hence reducing the cause of common mode disturbances.
4) Plates connected to chassis (as in standard power modules) will result in high current level circulating on external loom in an uncontrolled way, causing common-mode disturbances.

3.3 Sizing Y-Capacitors

Injected current will flows either through YCAPs or LISN, since in parallel. If the Y caps have lower impedance than those in the LISN, the CM noise current will be deviated from the LISN, not generating disturbance to the rest of the system. Thanks to the model developed, it has been possible to size these devices to make them effective, being aware of their maximum value given by safety considerations contained in ISO 6469 [17]. Moreover, it has been possible to find an unexpected issue: the noise level generated by the SiC inverter under test was above the expectances and it was producing excessive heat inside the Y capacitors. For this reason it was necessary to analyze further the phenomenon as described in [20].

3.4 Filter Design

Amongst all the analyses that can be done on a CM noise model, EMI filter design is probably the most valuable. Indeed, the possibility to study which path the injected current flows and estimating

the right input and output impedances of the circuit enable a more effective design of the filter and of all its components.
Obviously, the capability of modeling CM chokes is also required, but literature is full of these models with different level of details. If the model has to operate up to few hundreds MHz, a possible and simple implementation is described in [18].
This paper is not focusing on the filter design, but as sake of example Figure 8 shows the possible output of a parametric simulation where the CM noise generated by the model described in the previous sections has been compared with the same after the insertion of an AC and a DC filter respectively. Even if this model might be inaccurate because some stray component might be not correctly estimated or missing, it is immediately clear the advantage of having this kind of information in the early phase of the design of an electric vehicle drivetrain.
Other optimizations are possible, thanks to this approach; some of them are detailed into our previously published work on AC filtering [19] and thermal optimization of a DC EMI filter [21].

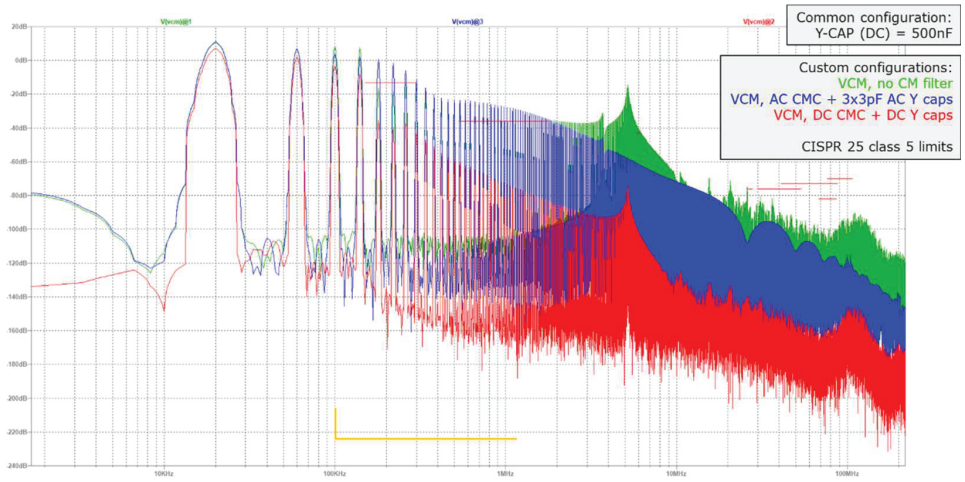

Figure 8: CM noise spectra in different model configuration: full model with two 500-nF Y-caps (green), the same model with an AC CM choke and Y-caps (blue), and the model with an optimized DC EMI filter (red).

4 Conclusion

This paper describes an approach to build a simplified SPICE model of an electric traction system in order to study the common-mode noise generation and propagation inside a vehicle. The approach can be applied to other domains, including industrial applications and energy distribution.
The model is based on coupling considerations of all the components of the system, i.e., the inverter, the motor, the wiring system. Each of these parts is studied to create a model that can be populated either with parameter extracted from other simulations or measurements from real samples. The combination of these components with the models of the LISN can make a SPICE circuit that can be simulated in few minutes to generate valuable results, like CM noise spectrum and current injected through the components of the system.
Parametric analysis can help finding the proper device to minimize the noise generation or propagation. Using the model, sizing the components of the filter is straightforward and can lead to very optimized design and even to find the proper configuration for a given setup.
This way to work enables a EMC-awareness in the early phase of design, leading to the consideration of EMC-related issues from the beginning, hence improving the design quality overall.

Literature

[1] IEC, “Vehicles, boats and internal combustion engines – Radio disturbance characteristics – Limits and methods for the protection of on-board receivers,” CISPR 25.
[2] IEC, “Vehicles, boats and internal combustion engines – Radio disturbance characteristics – Limits and methods of measurement for the protection of off-board receivers,” CISPR 12.
[3] A. Camarda, M. Balbarani, F. Calvano, S. Righi, L. Dossi, and A. Tacchini, “Characterization of High Voltage EMC filters for Electric Vehicles charging applications,” in 2023 International Symposium on Electromagnetic Compatibility, EMC Europe, 2023, pp. 1–6.
[4] C. Basso, “Spice predicts differential conducted EMI from switching power supplies,” 1997. http://powersimtof.com/Downloads/Divers/Predicting%20Differentiel%20EMI.pdf
[5] G. Brocard, The LTspice IV Simulator: Manual, Methods, and Applications. Wurth Electronics, 2013.
[6] P. Hillenbrand, S. Tenbohlen, C. Keller, and K. Spanos, “Understanding conducted emissions from an automotive inverter using a common-mode model,” in 2015 IEEE International Symposium on Electromagnetic Compatibility (EMC), 2015, pp. 685–690.
[7] D. N. Dalal, N. Christensen, A. B. Jorgensen, J. K. Jorgensen, S. Beczkowski, S. Munk-Nielsen, and C. Uhrenfeldt, “Impact of Power Module Parasitic Capacitances on Medium-Voltage SiC MOSFETs Switching Transients,” IEEE Journal of Emerging and Selected Topics in Power Electronics, vol. 8, no. 1, pp. 298–310, 2020.
[8] R. Martis, R. Siecoban, C. Martis, and S. Loránd, “Common and normal mode currents in PMSM PWM drives,” in SPEEDAM, 2016, pp. 500–504.
[9] J. Bjørngreen, “PMSM Diagnostics and Prognostics: Evaluation of an On-Line Method Based on High Frequency Current Response,” Ph.D. dissertation, Lund University, 2016.
[10] J.-k. Park, T. R. Wellawatta, S.-J. Choi, and J. Hur, “Mitigation Method of the Shaft Voltage According to Parasitic Capacitance of the PMSM,” IEEE Transactions on Industry Applications, vol. 53, no. 5, pp. 4441–4449, 2017.
[11] R. R. Riehl, J. A. Covolan Ulson, A. L. Andreoli, and A. F. Alves, “A simplified approach for identification of parasitic capacitances in three-phase induction motor driven by PWM inverter,” in 17th International Conference on Electrical Machines and Systems (ICEMS), 2014.
[12] T. Hadden, J. W. Jiang, B. Bilgin, Y. Yang, A. Sathyan, H. Dadkhah, and A. Emadi, “A Review of Shaft Voltages and Bearing Currents in EV and HEV Motors,” in IECON 2016 - 42nd Annual Conference of the IEEE Industrial Electronics Society, 2016, pp. 1578–1583.
[13] L. Ran, S. Gokani, J. Clare, K. Bradley, and C. Christopoulos, “Conducted electromagnetic emissions in induction motor drive systems. I. Time domain analysis and identification of dominant modes,” IEEE Transactions on Power Electronics, vol. 13, no. 4, pp. 757–767, 1998.
[14] X. Liu, “Methodology for EMC Analysis in a GaN Based Power Module,” Ph.D. dissertation, Universite Paris-Saclay, 2017.
[15] A. Oppenheim, R. Schafer, “Discrete-Time Signal Processing,” Pearson Education, 2013.
[16] J. Xue, “High Density EMI Filter Design in High Power Three-Phase Motor Drive System,” Ph.D. dissertation, University of Tennessee, 2014.
[17] International Standard Organization, “Electrically propelled road vehicles Safety specifications,” ISO 6469:2019.
[18] M. Tranchero and P. Santero, "A Simple SPICE Modeling Strategy for Common-Mode Chokes," *PCIM Europe 2022;* pp. 1-8, doi: 10.30420/565822212.
[19] M. Tranchero and P. Santero, “Comparison of AC Common-Mode Filter Topologies through SPICE Simulations,” in PCIM Europe 2023; pp. 1924-1929.
[20] M. Tranchero and P. Santero, "Thermal Considerations for Y Capacitors in Wide Band-Gap Based Inverters," *PCIM Europe 2023;* pp. 1-6, doi: 10.30420/566091349.
[21] M. Tranchero, P. Santero, G. Von Pfingsten and M. Nuotio, "Thermal Simulation and Optimization of a Common-Mode Filter for a SiC Inverter," 2023 International Symposium on Electromagnetic Compatibility – EMC Europe, Krakow, Poland, 2023, pp. 1-6.